

Are Low-Frequency Quasi-Periodic Oscillations seen in accretion flows the disk response to a jet instability?

J. Ferreira¹, G. Marcel², P.-O. Petrucci¹, J. Rodriguez³, J. Malzac⁴, R. Belmont³, M. Clavel¹, G. Henri¹, S. Corbel³, and M. Coriat⁴

¹ Univ. Grenoble Alpes, CNRS, IPAG, 38000 Grenoble, France

² Institute of Astronomy, University of Cambridge, Madingley Road, Cambridge, CB3 0HA, United Kingdom

³ AIM, CEA, CNRS, Université Paris-Saclay, Université de Paris, F-91191 Gif-sur-Yvette, France

⁴ IRAP, Université de Toulouse, CNRS, UPS, CNES, Toulouse, France

Received month dd, yyyy; accepted month dd, yyyy

ABSTRACT

Low Frequency Quasi-Periodic Oscillations or LF QPOs are ubiquitous in black hole X-ray binaries and provide strong constraints on the accretion-ejection processes. Although several models have been proposed so far, none has been proven to reproduce all observational constraints and no consensus has emerged yet.

We make the conjecture that disks in binaries are threaded by a large scale vertical magnetic field that splits it into two radial zones. In the inner Jet Emitting Disk (JED), a near equipartition field allows to drive powerful self-collimated jets, while beyond a transition radius, the disk magnetization is too low and a Standard Accretion Disk (SAD) is settled. In a series of papers, this hybrid JED-SAD disk configuration has been shown to successfully reproduce most multi-wavelength (radio and X-rays) observations, as well as the concurrence with the LFQPOs for the archetypal source GX 339-4.

We first analyze the main QPO scenarios provided in the literature: 1) a specific process occurring at the transition radius, 2) the accretion-ejection instability and 3) the solid-body Lense-Thirring disk precession. We recall their main assumptions and shed light on some severe theoretical issues that question the capability to reproduce LF QPOs. We then argue that none of these models could be operating under the JED-SAD physical conditions.

We finally propose an alternative scenario where LF QPOs would be the disk response to an instability triggered in the jets, near a magnetic recollimation zone. Such a situation could account for most Type-C QPO phenomenology and is consistent with the global behavior of black hole binaries. The calculation of this non-destructive jet instability remains however to be done. If the existence of this instability is numerically confirmed, then it could also naturally account for the jet wobbling phenomenology seen in various accreting sources, around compact objects and young forming stars.

Key words. Accretion, accretion discs – Magnetohydrodynamics (MHD) – X-rays: binaries – Galaxies: active – ISM: jets and outflows

1. Introduction

Black Hole X-ray Binaries (hereafter BH Xrb) are binary systems where a stellar-mass black hole accretes matter from a low-mass companion star. The incoming mass forms an accretion disk around the black hole which is detected mainly in X-rays. All systems are X-ray transients, spending sometimes years in a barely detectable quiescence and suddenly increasing their luminosity by factors up to 10^6 during months, until returning back to quiescence (see e.g. Remillard & McClintock 2006; Done et al. 2007; Dunn et al. 2010). These episodes of intense activity are accompanied by drastic spectral changes, with two main canonical spectral states. In the hard state, the spectrum is dominated by a (cut-off) power-law like emission usually attributed to inverse Comptonization that peaks at a few 100 keV and shows a quite intense (10 to 20% rms) rapid (subsecond) variability. In the soft state, the spectrum is characterized by a thermal black body emission of a few keV only and exhibits much less variability. A complete outbursting cycle can then be followed in a Hardness-Intensity Diagram (HID), where most BH sources make a q-shaped evolutionary track (see e.g. Dunn et al. 2010). Starting at low emission and in the hard state, an outburst consists first of a tremendous increase of luminosity in the hard state,

a sharp transition to a softer (low hardness) state while maintaining a roughly constant luminosity, followed by a luminosity decrease while remaining in this soft state, another transition back to the hard state at roughly the same luminosity and a final decay back the initial state (finishing the q-shape).

But the HID only probes accretion onto the black hole and does not convey all the phenomenology of these sources. It is now well known that jets, possibly in the form of bipolar self-confined outflows, are also emitted by the central regions. These jets are mainly detected in radio bands and show a clear correlation with the underlying X-ray emission, albeit only when the source is in the hard state (see e.g. Corbel et al. 2000, 2003, 2013; Gallo et al. 2003; Merloni et al. 2003; Falcke et al. 2004; Fender et al. 2004 and the review by Fender & Gallo 2014). While explaining only the behavior seen in the HID was already quite challenging *per se*, including the jet production mechanism (and its associated power leakage in the hard states) remains an open issue. There have been several propositions of course (e.g. Esin et al. 1997; Meyer-Hofmeister et al. 2005; Yuan et al. 2005; Ferreira et al. 2006b; Begelman & Armitage 2014; Kylafis & Beltoni 2015) but, to date, there is no clear consensus on which sce-

nario is the most likely to explain the complex multi-wavelength (radio to X-rays) time dependent behavior of BH XrBs.

The analysis of the fast timing variations seen in hard X-rays offers however another independent means to grasp the BH XRBs phenomenology (see Motta 2016; Ingram & Motta 2019 for recent reviews). The intrinsic variability of the sources is highly dependent of their spectral state, reaching 20% in the hard states, going down to 1-10% level in the hard-to-soft and soft-to-hard intermediate states and often consistent with zero in the soft state. Besides, the power density spectra have complex and state dependent shapes. On top of a broad band continuum, they can exhibit narrow features, called quasi-periodic oscillations or QPOs, of centroid frequency ν and extent $\Delta\nu$. There are three main types of low frequency ($\nu < 50$ Hz) QPOs that seem intimately linked to the spectral state (Remillard et al. 1999; Casella et al. 2004; Belloni et al. 2005): Type-C, the most common, are detected in hard states, Type-B appear during (and define) the intermediate states while Type-A are rare, only seen in the high soft state. Type-A QPOs are very weak and broad with $Q = \nu/\Delta\nu < 3$ and a frequency $\nu_A \sim 6 - 8$ Hz. Type-B QPOs are more prominent and narrow, with $Q \geq 6$ and $\nu_B \sim 1 - 6$ Hz. Finally, Type-C QPOs are strong and narrow, with $Q \geq 10$ and a frequency ν_C ranging from mHz to ~ 10 Hz.

Although there is a time sequence from one QPO type to another, it is not clear whether all types should be explained by the same model. For instance Type-B QPOs are stronger in more face-on objects and reveal a time proximity with transient radio flares, which has lead to propose a link between their appearance and the launching of discrete relativistic ejections (Fender et al. 2009; Motta et al. 2015; Stevens & Uttley 2016; Russell et al. 2019; Homan et al. 2020). But these two properties are not shared by all QPOs. Indeed, Type-A QPOs are detected in a jetless phase while Type-C QPOs are characterized by three extra properties (Remillard & McClintock 2006; Motta 2016). First, the frequency ν_C is independent of the energy band and source inclination, although always associated to the inner (hot) accretion flow (e.g van den Eijnden et al. 2017). Second, the time evolution of the QPO frequency is tightly correlated with the variation of the soft (< 10 keV) source count rate and hard X-ray power-law index, as well as the innermost radius of the cold (black body) accretion flow. However, the QPO frequencies are always much lower than the Keplerian frequency of the inner cold disk radius (e.g. Munro et al. 1999; Markwardt et al. 1999; Sobczak et al. 2000; Rodriguez et al. 2002; Vignarca et al. 2003; Rodriguez et al. 2004b; Remillard & McClintock 2006; Marcel et al. 2020). Finally, phase lags are also commonly observed between different energy bands (e.g. 2-5 versus 13-30 keV, Casella et al. 2004). The lag of a Type-C QPO is strongly correlated with its frequency and depends also on the object inclination: near zero but with an increasing hard lag (soft photons arriving first) with increasing QPO frequency for low inclination sources whereas high-inclination sources turn to soft lags at larger QPO frequencies (e.g. Motta et al. 2015; van den Eijnden et al. 2017; de Ruiter et al. 2019; Zhang et al. 2020; Ma et al. 2021).

Explaining Type-C LFQPOs is a challenging task and there have been already several models proposed in the literature. Yet, there is still no consensus as all QPO models are still facing major theoretical issues. Moreover, and more importantly, no model embraces the global picture of these accreting systems. Indeed, as intriguing as QPOs may be, they are only an epiphenomenon of the main accretion-ejection process. They must therefore be understood within, and be part of, a global framework that addresses also the other observational constraints

namely, spectral evolution, jet formation and quenching.

Hereafter, we focus on such a framework, the hybrid disk configuration proposed by Ferreira et al. (2006b), which has been recently successfully confronted to observations in a series of papers (Marcel et al. 2018b,a, 2019, 2020, 2022; Ursini et al. 2020; Marino et al. 2020; Barnier et al. 2022). In this framework, a large scale vertical magnetic field B_z is assumed to thread the inner disk regions, say below $10^4 r_g$ where $r_g = GM/c^2$ is the gravitational radius. At any given radius, its dynamical importance is measured at the disk midplane by the magnetization $\mu(r) = B_z^2/(\mu_o P_{tot})$, where P_{tot} is the sum of the gas and radiation pressure. It has been argued that this magnetization is a decreasing function of the radius and that the disk is separated into two distinct regions (Ferreira et al. 2006b; Petrucci et al. 2008). Beyond a transition radius r_J the magnetization is low and the disk is assumed to be in a Standard Accretion Disk (hereafter SAD) mode, where most of the disk angular momentum is carried radially away by a MRI-driven turbulence (Shakura & Sunyaev 1973; Balbus & Hawley 1991; Balbus 2003). Although winds are possible and even expected when a large scale B_z field is present, their influence on the disk energetics is rather small (Zhu & Stone 2018; Jacquemin-Ide et al. 2021). As a consequence, the SAD region accretes at a highly subsonic speed and is optically thick. On the contrary, the region below r_J and extending down to the innermost stable circular orbit r_{ISCO} is in a Jet Emitting Disk (hereafter JED) mode, where a sizable fraction of the disk angular momentum is carried away vertically by two self-confined magnetically-driven jets. The JED model is a generalization and an extension of the Blandford & Payne (1982) jet model, addressing both the mass loading issue and causal connection with the underlying disk. This inner JED region is characterized by a magnetic field near equipartition (a constant μ around 0.1–0.8), leading to a supersonic accretion speed (Ferreira & Pelletier 1995; Ferreira 1997). As a consequence, the JED region is much less dense than the outer SAD and becomes optically thin and geometrically slim.

As estimated in Marcel et al. (2018a), the radial JED-SAD transition is achieved when the inner disk magnetization in the SAD reaches a value $\mu_c \sim 10^{-3}$. This critical value triggers the inward radial transition to a JED and leads to a sudden drop in density and increase in accretion speed as the jet torque becomes dominant. Postulated in 2006, this radial JED-SAD disk configuration seems to be qualitatively consistent with current 3D global MHD simulations, both in non-relativistic (Jacquemin-Ide et al. 2021) and relativistic regimes (Igumenshchev et al. 2003; Tchekhovskoy et al. 2011; McKinney et al. 2012; Avara et al. 2016; Liska et al. 2020 to cite only a few)¹.

This framework allows to reproduce most of the available data for the archetypical source GX 339-4. Indeed, by allowing the disk accretion rate \dot{m} and the transition radius r_J to vary independently with time, 4 cycles of activity have been successfully reproduced (see Marcel et al. 2020 and references therein). It is remarkable that time evolutions of the pair (r_J, \dot{m}) are able to reproduce each individual spectra and the HID of GX 339-4,

¹ In GRMHD simulations, this inner zone has usually been termed a Magnetically Arrested Disk or MAD, a model initially defined as $B_z B_r^+/\mu_o \sim \rho \Omega_K^2 r h$, namely where the poloidal laminar magnetic field would be so strong that it would provide a support against gravity. Assuming $B_r^+ \sim B_z$, this requires a disk magnetization $\mu \sim r/h$ (see Narayan et al. 2003 and references therein). On the other hand, a JED is a sub-Keplerian disk with μ of order unity, enough to launch centrifugally-driven jets. More numerical efforts must be done to assess the differences between a JED and a MAD.

but also the radio emission (although in a more qualitative way). Moreover, it has been also firmly established that the frequency of the detected Type-C LFQPOs follows the scaling law

$$\nu_{QPO} = \nu_K(r_J)/\chi \quad (1)$$

where $\nu_K(r_J)$ is the keplerian orbital frequency at r_J and χ is a constant factor ~ 100 (actually varying from 70 to 130, depending on the outbursting cycle). This result, verified for more than two decades in frequencies, clearly advocates for a strong connexion between the physical source of the LFQPO and the transition radius r_J (Marcel et al. 2020).

To our knowledge, and despite several simplifications, this framework is currently the only one providing a clear picture addressing most of the observational accretion-ejection constraints. However, it is not clear yet if the observed timing properties, and in particular the LFQPOs, can fit inside this paradigm. This is the purpose of this paper.

We first critically analyze in section 2 the main QPO scenarios provided in the literature: a specific process triggered at the transition radius, the accretion-ejection instability (Tagger & Pellat 1999) and solid-body Lense-Thirring disk precession model (Ingram et al. 2009). We recall their main results but highlight also (sometimes severe) theoretical issues (see Ingram & Motta (2019); Marcel & Neilsen (2021) for observational issues). Putting these issues aside, it will be moreover argued that none of these scenarii can provide an explanation for Type-C QPOs fulfilling Eq.(1) within the JED-SAD framework. In section 3, we finally propose a novel scenario where the observed LFQPOs would be the inner JED response to a jet instability occurring away from the disk. It will be shown in Section 4 that such a situation not only provides a qualitative explanation for the LFQPO phenomenology, but it may also provide insights into the behavior of astrophysical jets. We conclude in section 5.

2. Comments on some models for LF QPOs

Before proposing a new scenario for the LFQPO (Sect. 3) we first discuss in this section several existing models. We only address those which, in our view, are the most representative in the literature and refer instead the interested reader to the reviews of Done et al. (2007) and Ingram & Motta (2019) for an exhaustive list. Note that all models require the existence of a transition radius usually associated to the innermost black body disk. When applicable, we discuss also some of these models in the context of the JED-SAD framework.

2.1. A specific process occurring at the transition radius

Since the QPO frequency in hard X-ray emission is tightly correlated with the transition radius (labelled r_J in the JED-SAD framework), it is natural to first look at a physical process that would be triggered at that specific location. The problem of course is the factor $\chi \sim 100$ which requires to look for a very slow, secular process.

It is known for instance that any misalignment between the black hole spin and the disk leads to a Lense-Thirring (hereafter LT) precession due to the dragging of inertial frames (see Bardeen & Petterson 1975 and references therein). As a consequence, a test particle located at a radius r from a black hole of dimensionless angular momentum j would undergo a relativistic precession at the LT-frequency $\nu_{LT}(r) \simeq \frac{jc}{\pi r_g} (r/r_g)^{-3}$ which is steeply decreasing with the distance. Proposed initially for kHz

QPOs in XrBs (Stella & Vietri 1998; Stella et al. 1999), one could also imagine that the outskirts of a hot inner flow, specifically a hot ring near the transition radius with the SAD, could provide an observable LFQPO. However, the ratio $\nu_{LT}/\nu_K(r_J) = 2j(r_J/r_g)^{-3/2} \propto r_J^{-3/2}$ keeps decreasing with the distance. This is in contradiction with the observational constraint Eq. (1), where this ratio remains roughly constant regardless of r_J .

Motivated by the similarity between the observed power-density spectra of BH XrBs and the response function to external perturbations of driven mechanical and electrical systems, Psaltis & Norman (2000) computed the response of a narrow (of $\delta r/r \sim 0.01$), geometrically thin accretion disk annulus to a broad spectrum of isothermal perturbations imposed outside of it. That ring corresponds to an abrupt change of disk properties, probably again the transition radius. They found that some resonances appear superimposed on the incoming spectrum, leading to observable QPOs. Since they neglected the radial pressure forces, the predicted mode frequencies depend mostly on the gravitational field around the compact object and only weakly on the hydrodynamic properties of the flow itself. As a result, the selected frequencies are related to the epicyclic and LT frequencies at the transition radius, which are both unable to explain LFQPOs due to the huge factor χ .

Kato & Manmoto (2000) proposed a model of trapped oscillations that would be triggered at the transition radius between the outer SAD and an inner Advection Dominated Accretion Flow or ADAF (Ichimaru 1977; Narayan & Yi 1994, see also the review by Yuan & Narayan 2014). Such a situation implies a very narrow transition zone where the rotation profile needs to become slightly super Keplerian (Abramowicz et al. 1998). As a consequence the epicyclic frequency κ^2 becomes negative, leading to a local instability (Rayleigh criterion, when the stabilizing effects due to the strong inhomogeneities are negligible). The authors then argue that the slowly growing amplitude of the perturbations would remain trapped around the transition radius, leading to local QPOs.

Assuming a particular radial profile for the disk temperature within the transition region, they solved the local dispersion relation of these inertial-acoustic modes. They showed that it is possible to fine-tune the radial profile so that the eigenvalue could match the QPO frequency at a given transition radius. However, and this is quite uncomfortable, this fine-tuning must be done for every radius and for a given set of disk parameters. It seems therefore difficult to reconcile this result with the generic behavior deduced from observations². Not only there is no reason why such a fine-tuning should occur, but the model relies also on strong approximations. Of particular importance is the neglect of the accretion motion, which would unavoidably lower the local growth of perturbations by advecting them.

This remark is even more critical within the JED-SAD framework, which assumes the presence of a large scale B_z field everywhere. Whether or not such an instability would be present near r_J in this case requires a novel investigation. However, the disk material undergoes a transsonic transition at r_J (Ferreira et al. 2006b; Marcel et al. 2018a; Scepi et al. 2019), since the SAD accretes at subsonic speeds whereas the JED is supersonic. Moreover, in order for a JED to maintain a constant disk magnetization μ , any extra magnetic flux that would be carried in by the accreting flow must be expelled out. This is exactly what happens in some GRMHD simulations, where a magnetic Rayleigh-

² This fine-tuning has nothing to do with a "p-disk model", which is a multi-blackbody disk model where the temperature exponent is left free (Mineshige et al. 1994; Kubota et al. 2005).

Taylor instability is seen to grow up and expel the magnetic flux excess as magnetic bubbles (McKinney et al. 2012; Marshall et al. 2018). Quite interestingly, this is done quasi-periodically but on a time scale comparable to a few Keplerian orbits at r_J , inconsistent with LFQPOs. The existence of such a messy, transonic JED-SAD transition casts therefore serious doubts on the possibility to allow the development of any secular instability at that location.

2.2. The accretion-ejection instability

The accretion-ejection instability (AEI) has been first studied by Tagger & Pellat (1999) in the context of accretion disks threaded by a large scale B_z field, and then proposed to explain QPOs by Varnière et al. (2002) and Rodriguez et al. (2002). A non-axisymmetric ideal MHD instability is found to be triggered whenever the vertical field reaches equipartition along with some radial profile. These spiral waves travel back and forth between the disk inner radius r_{in} (initially assumed to be the innermost SAD radius) and some radius r_{co} , defined as the co-rotation between the wave phase speed and the disk material rotation. The waves transport angular momentum outwardly, allowing the "cavity" between r_{in} and r_{co} to accrete rapidly. Although spiral waves are also emitted beyond r_{co} , accretion in this outer region is nevertheless assumed to carry on thanks to the usual MRI-driven turbulence. At the co-rotation radius, waves are evanescent but a resonance with a vertical Alfvén wave allows the transfer of some energy and angular momentum in the vertical direction. A magnetized azimuthally localized vortex is thus expected to grow at r_{co} , opening the possibility for some ejection there (but not demonstrated yet). Such a vortex is invoked to be the locus of enhanced dissipation (a hot spot), leading to a QPO with a frequency $\nu_K(r_{co})$, as long as some geometrical occultation is also present of course (so QPOs can be seen only in high inclination sources).

At first sight, the AEI would perfectly fit at the interface between the JED and SAD zones, due to the build-up of a large scale B_z field near equipartition in the JED. But in order for the AEI to reproduce the LFQPO behavior encapsulated in Eq. (1), the ratio of the co-rotation radius to the innermost disk radius (equal to r_J within the JED-SAD framework) must then be $\chi^{2/3} \gg 1$ (independent of r_J). Such a distance between the inner boundary and the co-rotation radius cannot be achieved within the AEI framework (see for instance Fig. 4 in Varnière et al. 2002). Indeed, as the magnetization increases, the wavelength becomes larger, widening the "cavity" and pushing out to larger radii the co-rotation radius. But this leads also to a widening of the forbidden zone around the corotation radius and the amplification mechanism becomes less efficient. As a result, the growth rate has a maximum for μ only close to 1 (Tagger & Pellat 1999). In other words, the factor $\chi \sim 100$ for Type-C QPOs cannot be achieved within the AEI framework for reasonable values of the magnetic field.

It must also be realized that the complex situation invoked for the AEI has been computed with a highly simplified setup so far. For instance, the toroidal component of the magnetic field has been neglected, which forbids of course the launching of jets and winds that would seriously affect the disk angular momentum transport. The unavoidable MRI-driven turbulence has been also discarded, while it provides both another torque and wave dissipation, two ingredients that would again lower the efficiency of the mechanism. On the other hand, despite the assumption of a perfect wave reflection at the inner disk boundary, the maximum AEI growth rate is already quite low, namely

of order $V_A/r \sim \mu^{1/2} \Omega_K h/r$ only (Tagger & Pellat 1999). This means that the physical ingredients listed above (jets, turbulence) would probably seriously lower it or even quench the instability. Finally, the probable presence of a magnetic Rayleigh-Taylor instability at the edge of the JED, as seen in MAD simulations (McKinney et al. 2012; Marshall et al. 2018) questions the very existence of the AEI at that location. Because of all these extra ingredients, assuming a perfectly reflecting boundary at r_J appears rather dubious indeed.

Given all these difficulties and in particular the unreachable factor χ , we think that AEI is very unlikely the source of Type-C QPOs within the JED-SAD framework. However, for Type-A and/or Type-B LFQPOs, that are observed only when r_J is near the ISCO and relativistic effects important (see Varnière et al. 2012 and references therein), the AEI may remain a possible candidate.

2.3. Solid-body Lense-Thirring disk precession model

The solid-body precession of the inner disk due to the Lense-Thirring effect is certainly the most popular model invoked to explain Type-C LFQPOs (Ingram et al. 2009; Ingram & Motta 2019). This model relies on a geometrical general relativity effect, occurring whenever the black hole spin is misaligned with the disk axis. The resulting frame drag causes important structural changes in the surrounding accretion disk (precession) as it struggles to adapt its equatorial plane to the periodic changes in the local gravitational field. The model of Ingram et al. (2009) for QPOs has been designed within the framework of Esin et al. (1997): an inner hot, optically thin and geometrically thick flow (ADAF) is settled until a transition radius r_t beyond which the disk becomes the usual cold, optically thick and geometrically thin SAD. Within this framework, a LFQPO correlated with r_t (hence also with the disk black body) could arise if the inner geometrically thick disk (ADAF) modulates the X-ray flux. But this can only happen if a significant portion of the ADAF's volume is precessing as a *solid body*, namely with a unique precession frequency ν_{prec} .

As shown by Ingram et al. 2009, if that volume extends down to the innermost stable orbit, not only the precession frequency ν_{prec} would exhibit a too strong dependence on the black hole spin, but it would also provide frequencies far too high. As a consequence, it is usually assumed that the innermost disk regions, up to a few r_g , are actually aligned with the black hole spin, probably due to a Bardeen-Petterson effect (Bardeen & Petterson 1975; Papaloizou & Lin 1995; Lubow et al. 2002). Alignment of the inner zone is actually always seen in all numerical simulations of tilted black holes (see e.g. Fragile et al. 2007; Fragile 2009), although the presence of large scale magnetic fields seems to seriously modify the estimate of this inner radius and even question the physical mechanism (McKinney et al. 2013; Krolik & Hawley 2015; Liska et al. 2018, 2019; Chatterjee et al. 2020; Liska et al. 2021). Nevertheless, assuming an inner radius of a few r_g and a solid-body LT-precession up to an arbitrary transition radius r_t , Ingram et al. (2009) have shown that the precession frequency $\nu_{prec}(r_t)$ could indeed cover the observed frequency range of Type-C QPOs from ~ 0.01 to ~ 10 Hz. Note that the actual value of ν_{prec} is a direct function of the external radius r_t , which remained a free parameter in this work. Several other observational features related to QPOs have been obtained within this framework (see the review of Ingram & Motta 2019).

However, as appealing as this scenario is, the proof that a solid-body LT-precession is settled over a significant radial range remains controversial in numerical GR simulations. In-

deed, while solid body precession has been clearly shown in hydrodynamical flows (see eg. Fragile & Anninos 2005; Dyda & Reynolds 2020), the trend is much less clear when magnetized flows are considered. There has been some works claiming that there is indeed a volume undergoing a solid-body LT-precession (e.g. Fragile et al. 2007; Liska et al. 2018, 2019) and others where no evidence has been found (eg. McKinney et al. 2013; Sorathia et al. 2013; Krolik & Hawley 2015; Chatterjee et al. 2020). The main reason of this discrepancy is probably the difference in the large scale magnetic field accumulated in the central disk regions (namely the value of the achieved disk magnetization μ). Indeed, not only a vertical field triggers an MRI-driven turbulence but it also launches jets from the disk. And it is well known that both effects, turbulence and jets, produce extra torques that may prevent the enforcement of solid-body precession by the Lense-Thirring torque (Sorathia et al. 2013; McKinney et al. 2013). It is also possible that high tilts (65°) would be able to tear off the inner disk up at a radius r_i and enforce a solid-body precession (Liska et al. 2021). However, it would be a rather strong implication of the model if, in order to reproduce LFQPOs, high tilts would always be required.

In any case, we would like to stress that providing the proof that a significant portion of the disk, say from $\sim 5r_g$ to $r_{out} \sim 20$ or even up to $100r_g$, is actually precessing as a solid-body is a formidable numerical task. It would require for instance to show that the local precession angle is the same for the whole range of radii, and that it evolves linearly in time such that $P(t) - P(0) = \dot{P}t$, with $\dot{P} = 2\pi\nu_{QPO}$ allowing to measure the QPO frequency (see e.g. Fig 2 in Dyda & Reynolds 2020). But this demands to maintain disk conditions at r_{out} (i.e. accretion rate) rather constant for a duration ΔT that must be at the very least 3 or 4 times the QPO period, namely $\Delta T \sim 1 - 3 (r_{out}/r_g)^{3/2} 10^3 r_g/c$. For instance, a 0.1 Hz QPO would require a converged simulation that would last for a few times $10^5 r_g/c$ for a 10 solar masses BH. While such long times have been recently achieved in a few simulations (e.g. Chatterjee et al. 2020; Liska et al. 2021), constant disk conditions in the outer regions are still not met (to our knowledge). This situation is due to the initial conditions, which do not include a steady outer accretion disk. It is therefore very difficult to assess whether a solid-body LT-precession is actually settled in and clearly deserves further numerical simulations, long enough and tailored to maintain an outer cold thin disk.

Notwithstanding these current difficulties, one could ask if this scenario could fit within our JED-SAD framework. It requires of course the black hole spin to be misaligned with the disk angular momentum vector, and there is no reason why it should not be (although large tilts are not expected to always be the rule). As a result of the LT-torque, the innermost disk region (up to a few r_g according to GRMHD simulations) should always be aligned with the BH spin, whether the disk is in a JED or in a SAD accretion mode (note however that this alignment may be modified from the usual Bardeen-Petterson mechanism by the presence of large scale magnetic fields Liska et al. 2019, 2021). But what happens then beyond this innermost aligned region, when there is an inner JED settled up to a large r_j ?

According to McKinney et al. (2013) and references therein, one can answer this question by comparing the LT-torque with the other local torques acting on the disk. The local LT torque acting on a disk annulus can be estimated as $\Gamma_{LT} = \Omega_{LT} L \sin\beta$, where Ω_{LT} is the LT-precession pulsation, $L = \Sigma \Omega_K r^2$ is the disk angular momentum per unit area and β the black hole tilt angle (see e.g. McKinney et al. 2013 and references therein). In a JED, the dominant torque is the magnetic braking provided by the two

jets and writes $\Gamma_{jets} = -2r \frac{B_\phi^+ B_z}{\mu_o}$, which leads to a ratio

$$\frac{\Gamma_{LT}}{\Gamma_{jets}} = \sin\beta \frac{2j}{q\mu} \frac{r}{h} \left(\frac{r}{r_g}\right)^{-3/2} \quad (2)$$

In this expression, $q = -B_\phi^+/B_z$ is the magnetic shear measured at the disk surface, μ is the disk magnetization measured at the disk midplane (note that it does not include turbulent fields) and h/r the local disk aspect ratio. Since a hot JED verifies $q\mu \sim 1$ and $h/r \sim 0.1$ (Marcel et al. 2018b), this expression shows that the LT torque should never be dominant in a JED beyond a few r_g . Please note that this conclusion stems only from our assumption of the existence of a near equipartition laminar magnetic field.

This result can also be understood in other terms. In order for a solid-body LT-precession to take place, the disk must behave as a whole entity. This situation requires that a strong causal connection is maintained between its two radial boundaries. Namely, that bending waves can propagate back and forth and enforce the same precession rate over the entire volume. This "wave-like" regime has been estimated in hydrodynamical situations to require $\alpha_v < h/r$, namely a turbulent Shakura-Sunyaev α_v parameter smaller than the disk aspect ratio (Papaloizou & Lin 1995; Lubow et al. 2002). Since MRI provides a scaling $\alpha_v \sim 10\mu^{1/2}$ (Salvesen et al. 2016), it shows that weakly magnetized ($\mu < 10^{-4}$), hot ($h/r > 0.2$) flows could be in this regime and undergo indeed a solid body LT-precession. This was the situation envisioned initially (with an ADAF as the hot inner flow) and possibly achieved in some weakly magnetized GRMHD numerical simulations. But a JED has a near equipartition field ($\mu \sim 1$) and accretes at supersonic speeds due to its dominant jet torque. This challenges any upstream wave propagation and certainly forbids thereby the establishment of a solid body LT-precession over its entire volume³.

How much of the JED volume, located beyond the innermost region aligned with the BH, could be actually undergoing a solid-body precession remains an open issue. We stress however that in order to recover the observational correlation encapsulated in Eq.(1), that volume should reach a radius $r_i \equiv r_j$, which is doubtful according to both the previous causal argument and torque estimates. In the case of high tilts leading to disk tearing at a radius r_i (Liska et al. 2021), this radius should then also coincide with the transition to an outer SAD accretion mode. Within our JED-SAD framework, it is unclear to us why r_j , which marks the transition from μ near unity in the JED to $\mu \sim 10^{-3}$ in the inner SAD, should always be coincident with the tearing radius r_i .

Note finally that Marcel & Neilsen (2021) reached a similar conclusion based only on observational constraints. Indeed, in order to reproduce the observed X-ray spectra during the most luminous hard states, the hot flow must accrete at sonic to supersonic speeds (see e.g. Marcel & Neilsen 2021; Kawamura et al. 2022), unreachable with typical viscous torques. Since Type-C

³ Note that the JED thermal balance calculations done by Marcel et al. (2018a) lead to a disk aspect ratio h/r varying slowing with the radius (consistent with both the ion and electronic temperature profiles). On the other hand and for simplicity, a constant accretion Mach number (larger than unity) has been assumed in the JED, consistent with self-similar calculations. In a more realistic situation one would expect also a varying accretion Mach number. However, observations do require a supersonic accretion flow throughout the hot accretion flow (Marcel & Neilsen 2021; Kawamura et al. 2022), which means that the accretion speed (hence the jet torque) must also adapt. Thus, although there is a caveat of our calculations here, we believe it does not affect the main arguments presented in this section.

QPOs are prevalent in these luminous states, they concluded that solid-body LT-precession is unlikely the driving mechanism.

The existence of a BH-aligned precessing inner JED region translates of course into an inner jet precession and could therefore contribute to produce Type-A and/or Type-B QPOs (Stevens & Uttley 2016; Liska et al. 2019, 2021; Kylafis et al. 2020; Ma et al. 2021). And it could also provide the geometrical effect that is invoked to explain the influence of the source inclination on both the QPO amplitude and lags (e.g. Motta et al. 2015; Heil et al. 2015; van den Eijnden et al. 2017). But according to the above discussion, we doubt that solid body LT-precession could be the generic physical mechanism responsible for Type-C QPOs in all XrBs and believe that another mechanism needs therefore to be found (see also Nathan et al. 2022).

3. LFQPOs as the disk signature of a jet instability

Type-C LFQPOs are detected in the hard energy band which is associated to a corona or hot inner flow (see however discussion in Rodriguez et al. 2004a, 2008), but their frequencies show a tight correlation with the inner standard accretion disk radius, which is the JED-SAD transition radius r_J in our view (Eq.1). The difficulty is to reconcile this correlation with a factor $\chi \sim 100$, which requires a secular process.

In the JED-SAD framework, two bipolar self-confined jets are magnetically launched from the inner JED. Thus, instead of looking for a secular instability within the disk itself, we propose that these QPOs are the disk response to some instability triggered in the jets themselves, away from the disk. This idea could naturally reconcile the Type-C QPOs' low frequency (long-term or large scales behavior) with their apparent link with the transition radius r_J . There are several aspects that must be considered: (i) How can a jet instability still impact the underlying disk? (ii) Why would it have an influence on the JED spectrum? (iii) What kind of jet instability would then be necessary?

3.1. Causal connection with the underlying disk

Let us first assume that jets launched below r_J are indeed prone to some global instability. Since jets are clearly observed up to large scales, this instability must not lead to jet disruption. We thus only require that its non-linear stage leads to some local plasma and electric current re-organisation, ending up mostly into jet wobbling. It is that wobbling that defines a frequency, which is then expected to be conveyed backwards to the disk through waves. If this instability is triggered in the causally connected jet region, namely before the Fast-Magnetosonic (FM) surface, then FM waves can indeed propagate upstream and reach the disk (on a time of the order of the Keplerian orbital time scale at r_J , e.g. Ferreira & Casse 2004) so that we expect them to lead only to some broad band noise. But much longer time and/or spatial scales must be at play in order to trigger Type-C QPOs.

We are thus lead to assume that this jet wobbling occurs beyond the FM surface. In that case, waves can no longer propagate upstream *within the jet*. However, the JED-SAD framework requires the existence of a large scale vertical field threading the whole accretion disk. Although the super-FM jet is defined with the magnetic flux threading the JED, there is still magnetic field around it, threading the SAD. Such a field defines a magnetic sheath inside which the inner jet is propagating (see sketch in Fig.1). This outer sheath being sub-FM (as for instance in the simulations of Murphy et al. 2010), waves can still propagate downwards and reach thereby the disk. The path followed

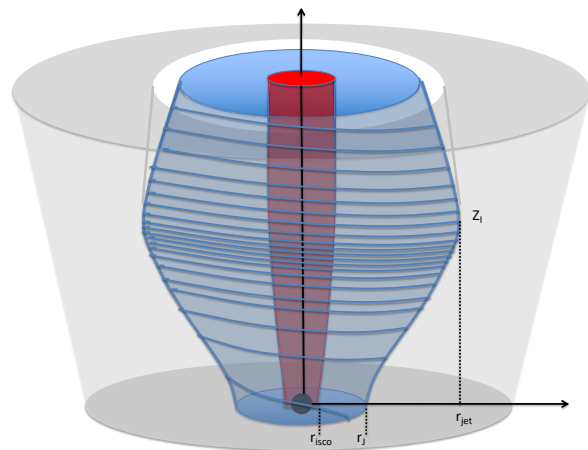


Fig. 1: Sketch of the JED-SAD hybrid disk configuration and its associated outflows in the hard state. The Jet Emitting Disk is settled from the ISCO r_{isco} up to the transition radius r_J , beyond which a Standard Accretion Disk is established. A vertical large scale magnetic field is threading the whole region, up to the axis. The red zone is the relativistic Blandford-Znajek spine, the blue zone is the sub to mildly relativistic Blandford-Payne jet launched from the JED and the grey shaded area is the outer magnetic sheath, with only unsteady sub-Alfvénic outflow (wind). The optimal location for the jet instability is the altitude z_I where the outer magnetic surface anchored at r_J is starting to recollimate toward the axis, defining the jet radius r_{jet} .

by these waves is not straightforward as the medium is inhomogeneous and waves are known to undergo some refraction. However, we expect modes to propagate preferentially along the sheath down to the transition radius r_J (much alike a surface mode). Moreover, once these waves reach the sub-FM zone of the inner jet, they will start to act as a lateral source localized at the limiting surface anchored at r_J . This will lead, in turn, to perturbations able this time to propagate within the jet and reaching the whole JED extension.

Our main assumption is therefore the existence of a jet instability triggered at a distance z_I leading to a subsequent jet wobbling. This lateral jet displacement bounces back on the magnetic sheath, which triggers the propagation of perturbations. How long it takes for these perturbations to reach the disk is a difficult question, as it requires to follow the path of these waves. Note however that once the instability is triggered, the perturbations in the jet itself are advected downstream, leaving behind the same physical conditions that have led to the triggering of the instability. As a consequence, it will grow again near z_I and lead to another unstable regime with a global jet displacement. As long as the conditions for the jet instability are met, one should thus see this going on, defining thereby a jet wobbling frequency ν_I which is mostly related to the time scale required for the lateral jet displacement. It is that frequency that will be observed as a LF QPO in the disk.

3.2. Impact on the accretion flow: LF QPOs

The jet instability acts like a hammer hitting the sheath with a characteristic frequency ν_I . The information (wobbling frequency and released energy) is transported backwards by FM waves travelling along the magnetic sheath surrounding the jet near r_J . A fraction of this energy is then expected to be spread

all over the JED, through a lateral "shower" of FM modes triggered at the magnetic sheath near the disk. How is that supposed to affect the emitted hard X-ray spectrum and lead to an observable LFQPO?

The fluctuations, typically 1-20% seen in hard X-rays, can be understood through two independent processes, both related to these incoming waves. Since they are FM waves, some vertical compression of the hot JED material is naturally expected, leading to some enhanced dissipation (thus emission) at the disk surface. The second aspect is related to the possible modifications of the jet torque acting upon the disk. These waves are indeed expected to introduce also fluctuations on the local toroidal magnetic field, hence on the torque due to the jet. As a consequence, one should see fluctuations of the JED accretion rate and on the related release of accretion energy, responding with the same quasi-periodic frequency ν_I .

However, to get a proper QPO with a rather large quality factor, one needs to have an almost resonant cavity. As shown by Cabanac et al. (2010), the JED itself may play this role, acting also as a low bandpass medium: its response to a white noise excitation is a flat-top noise power spectral density at low frequencies and a red noise at high frequency. In other words, if the jet acts like a hammer, the bell would be the JED⁴. A QPO is therefore expected to arise at a frequency ν_I , the same at each energy bin and related to the dynamical (epicyclic or keplerian) frequency at r_J (see below). It is however unclear how the existence of the outer magnetic sheath and intrinsic fluctuations of the dissipation within the JED will affect the calculations done by Cabanac et al. (2010). This should deserve further investigations.

3.3. Which instability could lead to jet wobbling ?

An MHD jet is a helical magnetic structure that can be seen as an ensemble of poloidal magnetic surfaces, nested around each other and in pressure equilibrium with the surrounding medium. In our JED-SAD framework, the jet is mostly the super-FM outflow emitted by the underlying JED established between the ISCO r_{isco} and r_J (blue region in Fig.1). Below r_{isco} , magnetic field lines are brought in and concentrated over the plunging region and black hole horizon (red region in Fig.1), leading to the production of a relativistic tenuous spine through the Blandford-Znajek process (Blandford & Znajek 1977). It is however unclear whether the existence of this spine has any dynamical impact on the outer Blandford-Payne jet. Indeed, radio observations can be accounted for using only the power carried by this outer flow component (Marcel et al. 2018a, 2019, 2020). But, in any case, if some jet instability is to give rise to a LFQPO related to r_J , it must involve the distant thus non-relativistic jet region. We thus neglect below the effect of the spine (see however Barnier et al. 2022).

Jets are prone to many instabilities such as pressure driven (PD), current driven (CD) and Kelvin-Helmholtz (KH) instabilities (plus any combination of them, Appl & Camenzind 1992; Baty & Keppens 2002, for a review see e.g. Hardee 2013). All these instabilities can either trigger radially localized, internal and surface modes or long-wavelength body modes. The final non-linear outcome of these instabilities can go from a simple internal redistribution of jet quantities (leading to a non-linear jet stabilization) to the production of internal shocks and/or MHD turbulence. In this latter case, a significant energy dissipation

⁴ This is somehow similar to the Psaltis & Norman (2000) approach: the hot inner JED acts as a filtering cavity of all incoming perturbations.

may eventually end up to a complete disruption of the jet on a finite distance. There is no consensus on which instability would be dominant in a jet as their existence and relative strength (growth rate) depend on the jet radial stratification, which is still poorly understood.

In this paper, we envision a non-destructive instability that gives birth to a long-wavelength instability at an altitude z_I , namely a global body-mode that involves lateral displacements of the whole outflow of radius r_{jet} . The jet radius r_{jet} is the radius achieved at z_I of the magnetic surface anchored at r_J . As discussed above, this displacement will bounce at the jet/magnetic sheath interface and trigger upstreaming (toward the disk) propagations of MHD disturbances. The jet displacement itself is advected downstream the flow and become potentially detectable farther out as jet wobbling. This allows another sequence (instability, jet displacement, bouncing) to set in at z_I , so that the whole process will be quasi-periodic with a characteristic frequency ν_I . The altitude z_I is therefore the lowest distance from the source where such an instability can take place. The frequency ν_I is related to the time scale involved for allowing FM waves to travel across the jet radius at z_I , so that it can behave as a whole (body mode). The frequency can thus be estimated as

$$\nu_I \sim \frac{V_{FM}}{2r} \Big|_{r_{jet}} \quad (3)$$

where V_{FM} is the FM phase speed at the jet radius r_{jet} . Assuming that the jet is cold and dominated by the toroidal magnetic field leads to

$$V_{FM} \simeq V_{A\phi} = \frac{B_\phi}{\sqrt{\mu_0 \rho}} = \frac{m}{m^2 - 1} \left(1 - \frac{r_A^2}{r^2} \right) \Omega_* r \simeq \frac{\Omega_* r}{m} \quad (4)$$

evaluated at $r = r_{jet} \gg r_J$ (Pelletier & Pudritz 1992). In this expression, $\Omega_* \simeq \Omega_K(r_J)$ is the angular velocity of the magnetic surface (MHD invariant), r_A is the Alfvén radius where the flow becomes super-Alfvénic and $m = u_p/V_{Ap}$ is the Alfvénic Mach number, assumed to be much larger than unity.

In order for the characteristic frequency ν_I to be identical to the LFQPO frequency ν_C , the condition

$$m \sim \pi \chi \quad (5)$$

on the Alfvénic Mach number m must be fulfilled, where we made use of Eq.(1). This is possible as long as magnetically driven jets from accretion disks are able to reach a value m between ~ 220 and 400 , for χ ranging from ~ 70 to 130 (Marcel et al. 2020). This is indeed the case, as shown for instance in Fig. 8 in Ferreira (1997). It corresponds to tenuous MHD solutions that become super-FM (namely $n = u_p/V_{FM}$ of a few) and that expand the most, with r_{jet}/r_J reaching values of a few hundreds up to a thousand (see his Fig.6). Note that Eq.(5) is not a fine tuning but instead a selection (and a property) of the underlying MHD solution established within the JED. The fact that such MHD solutions have been already computed is quite promising for our scenario.

Jets are highly inhomogeneous media, with both tremendous magnetic and velocity gradients whose effects on the development of an instability are not fully understood yet (see e.g. Bondeson et al. 1987; Birkinshaw 1991; Kersalé et al. 2000; Frank et al. 2000; Appl 1996; Mizuno et al. 2009, 2011, 2014; Kim et al. 2015, 2016, 2018). We note however that no instability is expected below the Alfvén surface. Indeed, the stabilizing magnetic tension due to the poloidal magnetic field is too important. Besides, just after the Alfvén point, MHD jets undergo

a huge lateral expansion leading to $|B_\phi| \gg B_p$ and $m \gg 1$, which reduces drastically the growth rate of any CD and KH modes, contrary to cylindrical jet configurations (see e.g. Rosen & Hardee 2000; Moll et al. 2008; McKinney & Blandford 2009; Porth & Komissarov 2015; Kim et al. 2016). We thus expect the triggering of CD or KH instabilities only at an altitude z_J where the jet radius has achieved some limiting value (i.e. a quasi-cylindrical jet), determined by the transverse equilibrium with its surrounding medium.

Our analysis points to the capital role played by the magnetic surface anchored at r_J . That surface corresponds to the last self-confined magnetic surface and thus to a maximum of the electric current flowing inside the jet. But since a sub-FM flow (probably even sub-Alfvénic) is expected to be established in the outer magnetic sheath (the grey portion of the magnetic flux anchored beyond r_J in Fig.1), a velocity shear is also necessarily present. Moreover, since the lateral equilibrium must be fulfilled, the outer (gas plus magnetic) pressure must balance both the inner jet ram pressure and magnetic deconfining force acting on the magnetic sheath. A density increase is thus to be expected in this region. These two elements (inner high speed jet surrounded by a denser and slower outflow) are very similar to those found at the spine-jet interface and clearly observed in GRMHD simulations. In accordance with our discussion, a CD kink instability leading to jet wobbling and wiggles is indeed seen to develop (see e.g. McKinney & Blandford 2009; Tchekhovskoy et al. 2011). Besides, the instability does not lead to jet destruction, probably because of the existence of this velocity shear (Mizuno et al. 2014; Kim et al. 2016, 2018).

We argued above that the optimal location for triggering a jet instability leading to jet wobbling would be the altitude z_J where the jet radius would reach its maximal size. This is a situation expected in self-similar Blandford-Payne jets and their generalization, as these type of jets always undergo a magnetic recollimation toward the axis (Contopoulos & Lovelace 1994; Ferreira 1997; Polko et al. 2010). Now, the existence of this intrinsic recollimation may cause a pressure mismatch at the jet-sheath interface (the white zone depicted in Fig.1), leading to a possible "recollimation" instability (Matsumoto & Masada 2013; Matsumoto et al. 2017). This new 3D instability, first associated to a Rayleigh-Taylor instability, is actually a variant of the centrifugal instability emerging along curved streamlines (Gourgouliatos & Komissarov 2018a,b). Whether it could lead to jet destruction and not only jet wobbling as assumed here remains to be fully assessed. However, it has been recently shown that it could be quenched with the presence of some external azimuthal magnetic field (Matsumoto et al. 2021).

As a final note, we remark that if we assume the recollimation point to be the locus of the jet instability, then the non-relativistic jet solutions that fulfill all constraints (super-FM, large radius and Eq.(5)) require a quite tiny mass loading parameter along that surface, namely a disk ejection efficiency ξ , defined as $\dot{M}_{acc} \propto r^\xi$ in the JED, satisfying $5 \cdot 10^{-3} < \xi < 10^{-2}$ (see Figs. 6 and 8 in Ferreira 1997). These values are consistent with jet speed estimates done for Cygnus X-1 (Petrucci et al. 2010). Note that this range stems from exact mathematical solutions but that more realistic ones should deviate from a strict self-similarity. Indeed, although the JED outermost magnetic surface should fulfill that constraint, the mass loading (or ejection index ξ) can increase progressively toward the center.

4. Discussion

4.1. Numerical simulations

Our wobbling jet scenario is quite generic and should therefore be observed in numerical jet simulations. However, as already pointed out, not only the physical conditions envisioned here are quite demanding but they also require full 3D simulations. Note that this jet wobbling should not be confused with jet precession due to the black hole tilt and leading to a Bardeen-Petterson like (probably modified by large scale magnetic fields) alignment of the innermost disk regions (McKinney et al. 2013; Liska et al. 2019, 2021). Although such precession may provide the correct physical ground for high frequency (kHz) QPOs, it cannot explain LF QPOs discussed here (see also Kylafis et al. 2020). Instead, we rely on a body mode instability in the super-FM regime, involving the whole jet radius and leading to quasi-periodic variations in the jet direction.

Although the stability of two-component magnetized jets are currently under study (see e.g. Millas et al. 2017 and references therein), they usually focus on the interplay between the inner relativistic spine and the outer slower and denser flow (usually referred to as the sheath in these works). We also note that with a much simpler jet profile, kink instabilities can indeed be obtained, affecting the large scale jet morphology and giving rise to interesting quasi-periodic radiative signatures (e.g. Tchekhovskoy & Bromberg 2016; Barniol Duran et al. 2017; Dong et al. 2020 see also the large scale 2D simulations of Chatterjee et al. 2019 showing pinch instabilities). However, we stress that a self-confined magnetized outflow must carry its own electric poloidal current and must therefore be seen as made of three components embedded in an external medium, not just two: the axial spine, the jet and the outer sheath.

In our view, the role of the central spine in the whole outflow collimation remains to be assessed (see for instance Barnier et al. 2022). The jet corresponds here to the super-FM Blandford-Payne outflow launched from the JED. The outer sheath is built up from the unavoidable magnetic flux threading the SAD region, which is settled beyond the JED. Note that such a magnetized sheath must be understood as being part of the whole outflow, since it must carry the return electric current (at the jet-sheath interface) that insulates the jet from the external medium (or cocoon). Understanding the propagation and stability properties of such stratified outflows is of great importance for accreting objects. But addressing both the large spatial and time scales involved, while also accounting for the complex jet stratification imposed by the underlying hybrid disk configuration, remains a numerical challenge.

4.2. Jet disruption and JED disappearance

Super-FM jets from JEDs are expected to start wobbling at some altitude z_J , but would they be disrupted? This is a difficult question to answer theoretically, as the non-linear saturation could be a simple readjustment of the gradients and the smearing out of the instability. There are for instance circumstances where a CD instability leads to the stabilisation of KH modes (Baty & Keppens 2002). Based on the observation that Type-C QPOs are maintained as long as there are steady compact jets (see however discussion in Fender et al. 2009; Fender & Gallo 2014), we assumed in our simplified picture that this instability is not leading to jet disruption. This requires that the jet is able to propagate up to a distance $L = xr_{jet}$ with, say x of a few hundreds, on a time $T = L/u_{p,max}$ shorter than the characteristic growth time of

the instability $\tau = \nu_J^{-1}$ (e.g. Kim et al. 2016). In this expression, $u_{p,max}$ is the maximum poloidal speed of the jet and is thus associated to the ISCO radius r_{isco} (for simplicity, we neglect here the effect of the fast spine). As a consequence, the instability will lead to jet destruction if $\tau < T$, which provides the condition $u_{p,max}/u_p(r_j) < x/2n$, where $n = u_p/V_{VM}$ is the FM Mach number measured at the outer jet region. This crude estimate shows right away that as $r_j \rightarrow r_{isco}$ it becomes harder to maintain stability: the thinner the jet and the more fragile, prone to destruction, it gets. This is qualitatively consistent for instance, with the fact that as the jet radius shrinks, the turbulent boundary layer due to a KH surface mode becomes of the order of the jet radius, leading thereby to its disruption (Baty & Keppens 2006; Kim et al. 2016). We thus expect a non-destructive jet wobbling whenever $r_j \gg r_{isco}$.

On the contrary, as the JED shrinks (hard-to-soft transition), the resulting jet would become too narrow to survive the instability. That would be coincident with a dramatic jet restructuring until its complete disruption and disappearance (assumed to occur at the "jet line"). However, before the complete jet disappearance, reconnecting events of the magnetic structure are expected to lead to the dramatic release of jet energy, possibly associated with discrete ejecta and subsequent radio flares (Homan et al. 2020; Wood et al. 2021).

These evidences of a link between the appearance of Type-B QPOs and the launch of discrete ejecta fits quite well within our jet instability scenario for QPOs. As $r_j \rightarrow r_{isco}$, we expect the jet to become also narrower due to the (relatively stronger) external magnetic pressure (Spruit et al. 1997). This translates into a QPO frequency $\nu_I \sim \Omega_K(r_j)/(2m)$ (Eq. 3) that could change while the transition radius r_j remains almost constant. Indeed, a smaller opening of the magnetic field lines leads to a smaller jet acceleration, hence to a smaller Alfvénic Mach number m . As a consequence, the QPO frequency may (slightly) increase while there is no detectable change in the inner cold disk radius (Kara et al. 2019; Ma et al. 2021). This is an aspect of jet collimation that has not been fully investigated yet.

4.3. Detectable signatures: IR QPOs, jet wobbling

Within the framework of wobbling jets, getting QPOs at the same frequency and at energy bands usually associated with jet emission (ie OIR) appears rather natural. Indeed, the jet instability is triggered at an altitude z_I (the recollimation zone) and gives rise to perturbations that propagate both up- and downstream. It will take a time Δt_X for the upstream waves to travel down to the disk and give rise to an observable QPO in the X-ray band. But since jet wobbling is quasi-periodically produced, it may well give rise to a OIR QPO at a distance $z_{IR} > z_I$ after a time $\Delta t_{IR} \sim (z_{IR} - z_I)/u_p$, where u_p is the flow speed (and possibly to some variability signature in radio bands Tetarenko et al. 2019). There is therefore no obvious reason why Δt_X should always be shorter than Δt_{IR} , so we do not expect any clear trend for the time lag between X and OIR QPOs (see also Veledina et al. 2013, 2015).

This is consistent with OIR QPOs lagging behind X-ray QPOs with ~ 0.1 sec in several XrBs (Gandhi et al. 2010; Kalamkar et al. 2016; Gandhi et al. 2017), but also with the non detection of any lag in MAXI J1535-571 (Vincentelli et al. 2021) or even X-rays possibly lagging behind the optical QPO in MAXI J1820+070 (Paice et al. 2021). Moreover, there are evidences of different properties between the two QPOs, like the rms-flux relation (Vincentelli et al. 2018) or the time evolution of the power spectral density (Vincentelli et al. 2019). Although

a common origin for X and OIR QPOs is quite natural within our framework, it seems plausible that some filtering effect is occurring as perturbations are propagating downstream the jet (see also Hynes et al. 2003).

Probing jet wobbling in BH XrB jets may be quite hard to achieve because of the lack of resolution (see however Miller-Jones et al. 2019). In the context of AGN, this requires instead a long term monitoring of jets. It is well known that AGN jets display non-radial motions, indicative of accelerated, non-ballistic motions (see e.g. Lister et al. 2016; Boccardi et al. 2017). But jet wobbling has been inferred in various BL Lac sources implying time scales from 2 to 20 yr (e.g. Agudo et al. 2012; Arshakian et al. 2020 and references therein). Walker et al. (2018) have also found evidences of such a pattern in the radio galaxy M87, with a period of ~ 9 yr. When scaled down to a 10 solar mass BH, this value provides a frequency around 2 Hz, which is consistent with the range of LF QPOs in BH XrBs.

In the realm of Young Stellar Objects, the situation is quite similar. Protostellar jets seen in the optical are thought to arise from the innermost disk regions, where orbital periods are ranging from few days to a year or so (Ferreira et al. 2006a; Ray et al. 2007 and references therein). On the other hand, these jets harbor knots that resemble bow shocks whose separations are indicative of time scales ranging from years to tens of years (e.g. López-Martín et al. 2003; Agra-Amboage et al. 2011; Ellerbroek et al. 2014; Lee et al. 2017; Tabone et al. 2017). Such time scales are too short to be explained by perturbations due to a companion star, and too long to be related to any dynamical time scale at the launching radius (see for instance jet wobbling in HH30, Louvet et al. 2018 and references therein). Instead of relating these knots to time variable ejection events from the source, we propose to relate them to the same jet instability. Such instability could be very similar to the one invoked here to explain LF QPOs around compact objects, although leading possibly to jet disruption with a subsequent ballistic motion in some sources.

5. Conclusion

Building upon the success of the JED-SAD framework to reproduce the radio emission and X-rays spectral energy distributions during various cycles of the archetypal source GX 339-4, we addressed in this paper the question of the origin of Type-C LFQPOs.

We first critically analyzed the most common models invoked for such QPOs: 1) models looking for a specific process triggered at the transition radius r_j , 2) the accretion-ejection instability and 3) the solid-body Lense-Thirring disk precession model. We showed that the first two types of models are facing major theoretical issues, unsolved yet, and that the published versions of these models do not account for the observed tight correlation with the disk transition radius (Eq. 1). We also argued that these models could not be operating within the JED-SAD framework.

We then discussed the case of the solid-body LT-precession model, which is invoked whenever the black hole spin is misaligned with the disk angular momentum vector. We argued that evidences in GRMHD simulations for such a solid-body behavior were not fully convincing, especially in the case of highly magnetized accretion flows. This casts thereby doubts on the capability of this model to operate within the JED-SAD framework (at least for moderate black hole tilts). As suggested however by current numerical simulations, the innermost JED region, up to a few r_g , would probably be aligned with the black hole spin, leading to an inner jet precession (namely a precession of both

the Blandford-Znajek axial spine and the innermost zones of the surrounding Blandford-Payne jet). But whether some fraction of the JED, located beyond the aligned region, would undergo a solid-body LT-precession remains an open issue that deserves further numerical simulations, long enough and tailored to maintain an outer cold thin disk. We argued however that such an effect would hardly be efficient up to the transition radius r_J with the outer SAD, as required by observations.

We propose instead that the JED-SAD framework offers the conditions allowing for a jet wobbling, namely a non-destructive long wavelength 3D body mode probably triggered by a kink or recollimation instability in the super-FM jet regime. Such a wobbling, triggered away from the disk, will nevertheless affect the disk through FM waves travelling upstream along the surrounding magnetic sheath, as well as, of course, downstream the jet. This outer magnetic sheath is the key ingredient allowing to connect the fast inner jet, which is hammering quasi-periodically against the sheath, to the underlying resonant disk (JED). This scenario offers thereby a unique explanation to the existence of QPOs seen both in disk (X-rays) and jet (UV and OIR) emission signatures.

The theoretical foundations of this scenario are threefold: i) existence of exact calculations of MHD accretion-ejection flows with the correct required properties; ii) self-consistent thermal disk balance calculations, with thorough confrontations to observations; iii) current knowledge on MHD instabilities in stratified super-FM flows. Notwithstanding these facts and hints, the proposed dynamical mechanism as well as its radiative consequences remain to be firmly established. To do so, global 3D jet simulations must be designed so that such an instability could be indeed observed, with its up-streaming perturbations heading toward the disk. On the radiative side, the work of Cabanac et al. (2010) should be extended in order to incorporate the existence of these incoming perturbations, and possibly address also the question of the time lags and their energy dependence.

We finally note that polarization measurements by IXPE, just launched in Dec. 2021 or, if selected, and in a more distant future, by eXTP, may bring great enlightenment on LFQPOs. Indeed, if swings in polarization angle are detected, this will provide stringent conditions that all the models and scenarios discussed above will have to explain. This is provided of course that such constraints are usable, as required integration times are much bigger than the periods to probe (but see for instance Ingram & Maccarone 2017).

Acknowledgements. JF would like to thank Adam Ingram and Matthew Liska, as well as the referee, Chris Done, for interesting discussions that allowed to improve the quality of the paper. We acknowledge financial support from the CNES French space agency and PNHE program of French CNRS.

References

Abramowicz, M. A., Igumenshchev, I. V., & Lasota, J.-P. 1998, *MNRAS*, 293, 443
 Agra-Amboage, V., Dougados, C., Cabrit, S., & Reunanen, J. 2011, *A&A*, 532, A59
 Agudo, I., Marscher, A. P., Jorstad, S. G., et al. 2012, *ApJ*, 747, 63
 Appl, S. 1996, *A&A*, 314, 995
 Appl, S. & Camenzind, M. 1992, *A&A*, 256, 354
 Arshakian, T. G., Pushkarev, A. B., Lister, M. L., & Savolainen, T. 2020, *A&A*, 640, A62
 Avara, M. J., McKinney, J. C., & Reynolds, C. S. 2016, *MNRAS*, 462, 636
 Balbus, S. A. 2003, *ARA&A*, 41, 555
 Balbus, S. A. & Hawley, J. F. 1991, *ApJ*, 376, 214
 Bardeen, J. M. & Petterson, J. A. 1975, *ApJ*, 195, L65
 Barnier, S., Petrucci, P. O., Ferreira, J., et al. 2022, *A&A*, 657, A11
 Barniol Duran, R., Tchekhovskoy, A., & Giannios, D. 2017, *MNRAS*, 469, 4957

Baty, H. & Keppens, R. 2002, *ApJ*, 580, 800
 Baty, H. & Keppens, R. 2006, *A&A*, 447, 9
 Begelman, M. C. & Armitage, P. J. 2014, *ApJ*, 782, L18
 Belloni, T., Homan, J., Casella, P., et al. 2005, *A&A*, 440, 207
 Birkinshaw, M. 1991, *MNRAS*, 252, 505
 Blandford, R. D. & Payne, D. G. 1982, *MNRAS*, 199, 883
 Blandford, R. D. & Znajek, R. L. 1977, *MNRAS*, 179, 433
 Boccardi, B., Krichbaum, T. P., Ros, E., & Zensus, J. A. 2017, *A&A Rev.*, 25, 4
 Bondeson, A., Iacono, R., & Bhattacharjee, A. 1987, *Physics of Fluids*, 30, 2167
 Cabanac, C., Henri, G., Petrucci, P., et al. 2010, *MNRAS*, 404, 738
 Casella, P., Belloni, T., Homan, J., & Stella, L. 2004, *A&A*, 426, 587
 Chatterjee, K., Liska, M., Tchekhovskoy, A., & Markoff, S. B. 2019, *MNRAS*, 490, 2200
 Chatterjee, K., Younsi, Z., Liska, M., et al. 2020, *MNRAS*, 499, 362
 Contopoulos, J. & Lovelace, R. V. E. 1994, *ApJ*, 429, 139
 Corbel, S., Coriat, M., Brocksopp, C., et al. 2013, *MNRAS*, 428, 2500
 Corbel, S., Fender, R. P., Tzioumis, A. K., et al. 2000, *A&A*, 359, 251
 Corbel, S., Nowak, M. A., Fender, R. P., Tzioumis, A. K., & Markoff, S. 2003, *A&A*, 400, 1007
 de Ruiter, I., van den Eijnden, J., Ingram, A., & Uttley, P. 2019, *MNRAS*, 485, 3834
 Done, C., Gierliński, M., & Kubota, A. 2007, *A&A Rev.*, 15, 1
 Dong, L., Zhang, H., & Giannios, D. 2020, *MNRAS*, 494, 1817
 Dunn, R. J. H., Fender, R. P., Körding, E. G., Belloni, T., & Cabanac, C. 2010, *MNRAS*, 403, 61
 Dyda, S. & Reynolds, C. S. 2020, arXiv e-prints, arXiv:2008.12381
 Ellerbroek, L. E., Podio, L., Dougados, C., et al. 2014, *A&A*, 563, A87
 Esin, A. A., McClintock, J. E., & Narayan, R. 1997, *ApJ*, 489, 865
 Falcke, H., Körding, E., & Markoff, S. 2004, *A&A*, 414, 895
 Fender, R. & Gallo, E. 2014, *Space Sci. Rev.*, 183, 323
 Fender, R. P., Belloni, T. M., & Gallo, E. 2004, *MNRAS*, 355, 1105
 Fender, R. P., Homan, J., & Belloni, T. M. 2009, *MNRAS*, 396, 1370
 Ferreira, J. 1997, *A&A*, 319, 340
 Ferreira, J. & Casse, F. 2004, *ApJ*, 601, L139
 Ferreira, J., Dougados, C., & Cabrit, S. 2006a, *A&A*, 453, 785
 Ferreira, J. & Pelletier, G. 1995, *A&A*, 295, 807
 Ferreira, J., Petrucci, P.-O., Henri, G., Saugé, L., & Pelletier, G. 2006b, *A&A*, 447, 813
 Fragile, P. C. 2009, *ApJ*, 706, L246
 Fragile, P. C. & Anninos, P. 2005, *ApJ*, 623, 347
 Fragile, P. C., Blaes, O. M., Anninos, P., & Salmonson, J. D. 2007, *ApJ*, 668, 417
 Frank, A., Lery, T., Gardiner, T. A., Jones, T. W., & Ryu, D. 2000, *ApJ*, 540, 342
 Gallo, E., Fender, R. P., & Pooley, G. G. 2003, *MNRAS*, 344, 60
 Gandhi, P., Bachetti, M., Dhillon, V. S., et al. 2017, *Nature Astronomy*, 1, 859
 Gandhi, P., Dhillon, V. S., Durant, M., et al. 2010, *MNRAS*, 407, 2166
 Gourgouliatos, K. N. & Komissarov, S. S. 2018a, *Nature Astronomy*, 2, 167
 Gourgouliatos, K. N. & Komissarov, S. S. 2018b, *MNRAS*, 475, L125
 Hardee, P. E. 2013, in *European Physical Journal Web of Conferences*, Vol. 61, The Innermost Regions of Relativistic Jets and Their Magnetic Fields, ed. J. L. Gómez
 Heil, L. M., Uttley, P., & Klein-Wolt, M. 2015, *MNRAS*, 448, 3348
 Homan, J., Bright, J., Motta, S. E., et al. 2020, *ApJ*, 891, L29
 Hynes, R. I., Haswell, C. A., Cui, W., et al. 2003, *MNRAS*, 345, 292
 Ichimaru, S. 1977, *ApJ*, 214, 840
 Igumenshchev, I. V., Narayan, R., & Abramowicz, M. A. 2003, *ApJ*, 592, 1042
 Ingram, A., Done, C., & Fragile, P. C. 2009, *MNRAS*, 397, L101
 Ingram, A. R. & Maccarone, T. J. 2017, *MNRAS*, 471, 4206
 Ingram, A. R. & Motta, S. E. 2019, *New A Rev.*, 85, 101524
 Jacquemin-Ide, J., Lesur, G., & Ferreira, J. 2021, *A&A*, 647, A192
 Kalamkar, M., Casella, P., Uttley, P., et al. 2016, *MNRAS*, 460, 3284
 Kara, E., Steiner, J. F., Fabian, A. C., et al. 2019, *Nature*, 565, 198
 Kato, S. & Manmoto, T. 2000, *ApJ*, 541, 889
 Kawamura, T., Axelsson, M., Done, C., & Takahashi, T. 2022, arXiv e-prints, arXiv:2107.12517
 Kersalé, E., Longaretti, P. Y., & Pelletier, G. 2000, *A&A*, 363, 1166
 Kim, J., Balsara, D. S., Lyutikov, M., & Komissarov, S. S. 2016, *MNRAS*, 461, 728
 Kim, J., Balsara, D. S., Lyutikov, M., & Komissarov, S. S. 2018, *MNRAS*, 474, 3954
 Kim, J., Balsara, D. S., Lyutikov, M., et al. 2015, *MNRAS*, 450, 982
 Krolik, J. H. & Hawley, J. F. 2015, *ApJ*, 806, 141
 Kubota, A., Ebisawa, K., Makishima, K., & Nakazawa, K. 2005, *ApJ*, 631, 1062
 Kylafis, N. D. & Belloni, T. M. 2015, *A&A*, 574, A133
 Kylafis, N. D., Reig, P., & Papadakis, I. 2020, *A&A*, 640, L16
 Lee, C.-F., Ho, P. T. P., Li, Z.-Y., et al. 2017, *Nature Astronomy*, 1, 0152
 Liska, M., Hesp, C., Tchekhovskoy, A., et al. 2018, *MNRAS*, 474, L81
 Liska, M., Hesp, C., Tchekhovskoy, A., et al. 2021, *MNRAS*, 507, 983
 Liska, M., Tchekhovskoy, A., Ingram, A., & van der Klis, M. 2019, *MNRAS*, 487, 550

- Liska, M., Tchekhovskoy, A., & Quataert, E. 2020, *MNRAS*, 494, 3656
- Lister, M. L., Aller, M. F., Aller, H. D., et al. 2016, *AJ*, 152, 12
- López-Martín, L., Cabrit, S., & Dougados, C. 2003, *A&A*, 405, L1
- Louvet, F., Dougados, C., Cabrit, S., et al. 2018, *A&A*, 618, A120
- Lubow, S. H., Ogilvie, G. I., & Pringle, J. E. 2002, *MNRAS*, 337, 706
- Ma, X., Tao, L., Zhang, S.-N., et al. 2021, *Nature Astronomy*, 5, 94
- Marcel, G., Cangemi, F., Rodriguez, J., et al. 2020, *A&A*, 640, A18
- Marcel, G., Ferreira, J., Clavel, M., et al. 2019, *A&A*, 626, A115
- Marcel, G., Ferreira, J., Petrucci, P.-O., et al. 2022, arXiv e-prints [arXiv:2109.13592]
- Marcel, G., Ferreira, J., Petrucci, P.-O., et al. 2018a, *A&A*, 617, A46
- Marcel, G., Ferreira, J., Petrucci, P.-O., et al. 2018b, *A&A*, 615, A57
- Marcel, G. & Neilsen, J. 2021, *ApJ*, 906, 106
- Marino, A., Malzac, J., Del Santo, M., et al. 2020, *MNRAS*, 498, 3351
- Markwardt, C. B., Swank, J. H., & Taam, R. E. 1999, *ApJ*, 513, L37
- Marshall, M. D., Avara, M. J., & McKinney, J. C. 2018, *MNRAS*, 478, 1837
- Matsumoto, J., Aloy, M. A., & Perucho, M. 2017, *MNRAS*, 472, 1421
- Matsumoto, J., Komissarov, S. S., & Gourgouliatos, K. N. 2021, *MNRAS*, 503, 4918
- Matsumoto, J. & Masada, Y. 2013, *ApJ*, 772, L1
- McKinney, J. C. & Blandford, R. D. 2009, *MNRAS*, 394, L126
- McKinney, J. C., Tchekhovskoy, A., & Blandford, R. D. 2012, *MNRAS*, 423, 3083
- McKinney, J. C., Tchekhovskoy, A., & Blandford, R. D. 2013, *Science*, 339, 49
- Merloni, A., Heinz, S., & di Matteo, T. 2003, *MNRAS*, 345, 1057
- Meyer-Hofmeister, E., Liu, B. F., & Meyer, F. 2005, *A&A*, 432, 181
- Millas, D., Keppens, R., & Meliani, Z. 2017, *MNRAS*, 470, 592
- Miller-Jones, J. C. A., Tetarenko, A. J., Sivakoff, G. R., et al. 2019, *Nature*, 569, 374
- Mineshige, S., Hirano, A., Kitamoto, S., Yamada, T. T., & Fukue, J. 1994, *ApJ*, 426, 308
- Mizuno, Y., Hardee, P. E., & Nishikawa, K.-I. 2011, *ApJ*, 734, 19
- Mizuno, Y., Hardee, P. E., & Nishikawa, K.-I. 2014, *ApJ*, 784, 167
- Mizuno, Y., Lyubarsky, Y., Nishikawa, K.-I., & Hardee, P. E. 2009, *ApJ*, 700, 684
- Moll, R., Spruit, H. C., & Obergaulinger, M. 2008, *A&A*, 492, 621
- Motta, S. E. 2016, *Astronomische Nachrichten*, 337, 398
- Motta, S. E., Casella, P., Henze, M., et al. 2015, *MNRAS*, 447, 2059
- Muno, M. P., Morgan, E. H., & Remillard, R. A. 1999, *ApJ*, 527, 321
- Murphy, G. C., Ferreira, J., & Zanni, C. 2010, *A&A*, 512, 82
- Narayan, R., Igumenshchev, I. V., & Abramowicz, M. A. 2003, *PASJ*, 55, L69
- Narayan, R. & Yi, I. 1994, *ApJ*, 428, L13
- Nathan, E., Ingram, A., Homan, J., et al. 2022, arXiv e-prints, arXiv:2201.01765
- Paice, J. A., Gandhi, P., Shahbaz, T., et al. 2021, *MNRAS*, 505, 3452
- Papaloizou, J. C. B. & Lin, D. N. C. 1995, *ApJ*, 438, 841
- Pelletier, G. & Pudritz, R. E. 1992, *ApJ*, 394, 117
- Petrucci, P. O., Ferreira, J., Henri, G., Malzac, J., & Foellmi, C. 2010, *A&A*, 522, A38
- Petrucci, P.-O., Ferreira, J., Henri, G., & Pelletier, G. 2008, *MNRAS*, 385, L88
- Polko, P., Meier, D. L., & Markoff, S. 2010, *ApJ*, 723, 1343
- Porth, O. & Komissarov, S. S. 2015, *MNRAS*, 452, 1089
- Psaltis, D. & Norman, C. 2000, arXiv e-prints, astro-ph/0001391
- Ray, T., Dougados, C., Bacciotti, F., Eislöffel, J., & Chrysostomou, A. 2007, in *Protostars and Planets V*, ed. B. Reipurth, D. Jewitt, & K. Keil, 231–244
- Remillard, R. A. & McClintock, J. E. 2006, *ARA&A*, 44, 49
- Remillard, R. A., Morgan, E. H., McClintock, J. E., Bailyn, C. D., & Orosz, J. A. 1999, *ApJ*, 522, 397
- Rodriguez, J., Corbel, S., Hannikainen, D. C., et al. 2004a, *ApJ*, 615, 416
- Rodriguez, J., Corbel, S., Kalemci, E., Tomsick, J. A., & Tagger, M. 2004b, *ApJ*, 612, 1018
- Rodriguez, J., Hannikainen, D. C., Shaw, S. E., et al. 2008, *ApJ*, 675, 1436
- Rodriguez, J., Varnière, P., Tagger, M., & Durouchoux, P. 2002, *A&A*, 387, 487
- Rosen, A. & Hardee, P. E. 2000, *ApJ*, 542, 750
- Russell, T. D., Tetarenko, A. J., Miller-Jones, J. C. A., et al. 2019, *ApJ*, 883, 198
- Salvesen, G., Simon, J. B., Armitage, P. J., & Begelman, M. C. 2016, *MNRAS*, 457, 857
- Scepi, N., Dubus, G., & Lesur, G. 2019, *A&A*, 626, A116
- Shakura, N. I. & Sunyaev, R. A. 1973, *A&A*, 24, 337
- Sobczak, G. J., McClintock, J. E., Remillard, R. A., et al. 2000, *ApJ*, 544, 993
- Sorathia, K. A., Krolik, J. H., & Hawley, J. F. 2013, *ApJ*, 777, 21
- Spruit, H. C., Foglizzo, T., & Stehle, R. 1997, *MNRAS*, 288, 333
- Stella, L. & Vietri, M. 1998, *ApJ*, 492, L59
- Stella, L., Vietri, M., & Morsink, S. M. 1999, *ApJ*, 524, L63
- Stevens, A. L. & Uttley, P. 2016, *MNRAS*, 460, 2796
- Tabone, B., Cabrit, S., Bianchi, E., et al. 2017, *A&A*, 607, L6
- Tagger, M. & Pellat, R. 1999, *A&A*, 349, 1003
- Tchekhovskoy, A. & Bromberg, O. 2016, *MNRAS*, 461, L46
- Tchekhovskoy, A., Narayan, R., & McKinney, J. C. 2011, *MNRAS*, 418, L79
- Tetarenko, A. J., Casella, P., Miller-Jones, J. C. A., et al. 2019, *MNRAS*, 484, 2987
- Ursini, F., Petrucci, P. O., Bianchi, S., et al. 2020, *A&A*, 634, A92
- van den Eijnden, J., Ingram, A., Uttley, P., et al. 2017, *MNRAS*, 464, 2643
- Varnière, P., Rodriguez, J., & Tagger, M. 2002, *A&A*, 387, 497
- Varnière, P., Tagger, M., & Rodriguez, J. 2012, *A&A*, 545, A40
- Veledina, A., Poutanen, J., & Ingram, A. 2013, *ApJ*, 778, 165
- Veledina, A., Revnivtsev, M. G., Durant, M., Gandhi, P., & Poutanen, J. 2015, *MNRAS*, 454, 2855
- Vignarca, F., Migliari, S., Belloni, T., Psaltis, D., & van der Klis, M. 2003, *A&A*, 397, 729
- Vincentelli, F. M., Casella, P., Maccarone, T. J., et al. 2018, *MNRAS*, 477, 4524
- Vincentelli, F. M., Casella, P., Petrucci, P., et al. 2019, *ApJ*, 887, L19
- Vincentelli, F. M., Casella, P., Russell, D. M., et al. 2021, *MNRAS*, 503, 614
- Walker, R. C., Hardee, P. E., Davies, F. B., Ly, C., & Junor, W. 2018, *ApJ*, 855, 128
- Wood, C. M., Miller-Jones, J. C. A., Homan, J., et al. 2021, *MNRAS*, 505, 3393
- Yuan, F., Cui, W., & Narayan, R. 2005, *ApJ*, 620, 905
- Yuan, F. & Narayan, R. 2014, *ARA&A*, 52, 529
- Zhang, L., Méndez, M., Altamirano, D., et al. 2020, *MNRAS*, 494, 1375
- Zhu, Z. & Stone, J. M. 2018, *ApJ*, 857, 34